# Electrode Resistance Effects in Interdigital Transducers

KENNETH M. LAKIN, MEMBER, IEEE

*Abstract*—A distributed *RC* circuit model is used to describe an interdigital electrode transducer (IDT) having finite conduction in the electrode stripes. The distributed circuit is described by a set of differential equations whose solutions yield the current and voltage distributions along the aperture of the IDT. It is found that the electrode resistance causes a distortion of the excited wave amplitude and phase due to the nonuniform voltage and current distribution. An equivalent circuit for the terminal properties is also derived which illustrates the effects of conduction loss. The theory is also used to predict electrode efficiency, effective aperture weighting, and phase shift in weighted arrays.

## I. INTRODUCTION

INTERDIGITAL electrode arrays for use in surface acoustic wave generation and detection are composed of thin films of conducting materials. The conducting material is usually chosen for its conductivity properties and to a lesser extent its acoustic properties. However, the electrode metallization does alter the wave propagation through a change in the surface wave velocity due to short circuiting of tangential electric fields [1], [2] and also introduces dispersion if the metallized layer has finite thickness [3]. Whereas the $\Delta v/v$ effect is always present, various materials may be chosen to acoustically match the substrate in order to minimize the effects of dispersion [4]. Some of the metals of interest have a lower bulk conductivity than copper, gold, or aluminum and therefore more electrode conduction loss would be expected. In addition, the net conductivity of a metallized layer depends upon the layer thickness which is usually chosen as thin as possible to avoid acoustic discontinuities, especially at microwave frequencies.

It is the purpose of this paper to describe a theoretical analysis of the effects of metallization sheet resistance upon the electrical properties of interdigital arrays. From the theoretical results a criterion may be established as to how large a sheet resistance could be employed and still avoid excessive conduction losses and beam amplitude and phase distortion. No attempt is made to correlate sheet resistance with a given metal's thickness because thin-film sheet resistance is highly dependent upon the method of film fabrication and specific metal. A few substrate materials are used as examples to illustrate the dependence upon material parameters and electrode equivalent circuit.

Manuscript received June 22, 1973; revised November 5, 1973. This work was supported by the Air Force Office of Scientific Research under Contract AFOSR-72-2391 and the Joint Services Electronics Program under Contract AFOSR F44620-71-C-0067.

The author is with the Electronic Sciences Laboratory, School of Engineering, University of Southern California, Los Angeles, Calif. 90007.

## II. THEORETICAL ANALYSIS

### A. Distributed Network Model

In order to accurately predict the effects of finite series resistance in IDT electrodes the structure will be analyzed as a distributed $R,C$ network as shown in Fig. 1. The electrode configuration for one finger pair is shown in Fig. 1(a) along with the assumed source current $I$ and coordinate system centered in the aperture $w$. A small incremental section of the aperture $\Delta x$ is defined and its equivalent electrical network is shown in Fig. 1(b). The relevant electrical parameters are the following:

- $\rho_c$ electrode resistance, ohms/(wavelength, $\lambda_0$);
- $y$ shunt admittance, mhos/(wavelength, $\lambda_0$);
- $i(x)$ upper electrode current;
- $i'(x)$ lower electrode current;
- $v(x)$ voltage between adjacent regions of the upper and lower electrodes.

If there is no acoustic wave generation, $y$ then corresponds to the incremental electrode capacitance. With acoustic generation, $y$ includes a radiation conductance $g$.

The model employs a current source rather than a terminal voltage for ease of analysis. However, eventually, the results will be expressed in terms of electrode voltage since finger pairs are usually connected in parallel but need not have the same current in the presence of aperture or phase weighting. Inductive effects between electrodes are

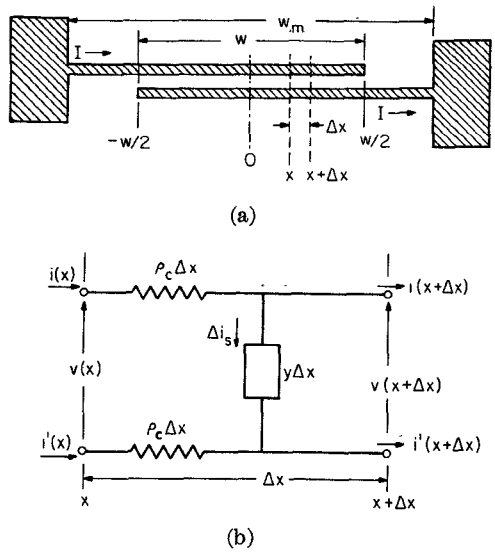


Fig. 1. Electrode pair and circuit model. (a) A one-electrode pair interdigital transducer with aperture $w$ having an input current from the left of $I$. (b) The equivalent circuit of a differential length $\Delta x$ and associated voltages and currents.

ignored because of the small physical dimensions usually employed in these structures.

### B. Network Equations

The analysis of the circuit of Fig. 1(b) follows from elementary circuit theory. However, it must be emphasized that the network is four-terminal but *not* a two-port. Since $i(x)$ is in general not equal to $i'(x)$ the usual transmission line equations cannot be applied. Nevertheless, differential equations for the currents and voltage may be derived in the usual manner from the network:

$$\frac{v(x+\Delta x)-v(x)}{\Delta x} = \rho_c[i'(x)-i(x)]$$

and

$$\frac{\Delta i_s}{\Delta x} = yv(x+\Delta x). \tag{1}$$

In the limit of small $\Delta x$ these equations reduce to

$$\frac{dv(x)}{dx} = \rho_c[i'(x)-i(x)]$$

$$\frac{di_s}{dx} = yv(x). \tag{2}$$

It is also apparent that

$$\frac{di_s}{dx} = -\frac{di}{dx} = \frac{di'}{dx} \tag{3}$$

from Kirchhoff's current law.

Using conservation of charge (current continuity) and the known boundary conditions, the relation between $i(x)$ and $i'(x)$ is obtained:

$$i(x)+i'(x) = I \tag{4}$$

where

$$i\left(-\frac{w}{2}\right) = I$$

$$i'\left(+\frac{w}{2}\right) = I$$

$$i\left(+\frac{w}{2}\right) = 0$$

$$i'\left(-\frac{w}{2}\right) = 0. \tag{5}$$

### C. General Solutions

By differentiating (1) and (2) and using relations (3) and (4) the following second-order equations are obtained:

$$\frac{d^2i(x)}{dx^2} - \alpha^2 i(x) = -\frac{\alpha^2 I}{2} \tag{6}$$

$$\frac{d^2v(x)}{dx^2} - \alpha^2 v(x) = 0 \tag{7}$$

where

$$\alpha^2 = 2\rho_c y. \tag{8}$$

For convenience $\alpha$ may be written as

$$\alpha = \left[\frac{8\rho_s}{\rho_a(1+Q_a^2)^{1/2}}\right]^{1/2} e^{j\theta}$$

where

- $\theta$ $= \frac{1}{2}\tan^{-1}(Q_a)$;
- $\rho_a$ radiation resistance in $\Omega\cdot\lambda$ (ohm-wavelength);
- $\rho_s$ sheet resistance in $\Omega/\square$ (ohms per square);
- $Q_a$ $\triangleq x_a/\rho_a$ = radiation $Q$ for single finger pair;
- $x_a$ series reactance in $\Omega\cdot\lambda$ (ohm-wavelength).

Since $Q_a$ is usually of order 10 or greater, the phase angle of $\alpha$ is nearly 45° and hence $\alpha$ has nearly equal real and imaginary parts. Since $Q_a$ is usually large $|\alpha|$ becomes for most cases

$$|\alpha| = \left[\frac{8\rho_s}{x_a}\right]^{1/2}.$$

Here $x_a$ is independent of transducer center frequency and essentially represents the capacitive reactance for one wavelength aperture. Thus $|\alpha|$ is directly proportional to the square root of the effective dielectric constant of the substrate. The phase factor $\alpha$ may be approximated by

$$\alpha \simeq \left(\frac{4\rho_s}{x_a}\right)^{1/2}(1+j).$$

Values for $\rho_a$, $Q_a$, $\theta$, and $|\alpha|$ are given in Table I for several materials. The values for $\rho_a$ and $Q_a$ were derived from an equivalent circuit model [5] as

$$\rho_a = (2\pi c V_s Q_a)^{-1}$$

$$Q_a = \left(\frac{8}{\pi}\Delta_0\right)^{-1}$$

where

- $\Delta_0$ open-circuit to short-circuit velocity parameter [2];
- $c$ single electrode capacitance/centimeter;
- $V_s$ surface wave velocity, centimeters per second.

TABLE I

| Material [6] | $\rho_a$, $\Omega\cdot\lambda$ | $Q_a$ | $\theta$, deg. | $\lvert\alpha\rvert$, $\rho_s = 1$ |
|---|---|---|---|---|
| ST Quartz | 1800 | 361 | 44.9 | $3.51 \times 10^{-3}$ |
| (010), [110] $Bi_{12}GeO_{20}$ | 4240 | 56.9 | 44.5 | $5.76 \times 10^{-3}$ |
| YZ $LiNbO_3$ | 7340 | 15.8 | 43.2 | $8.3 \times 10^{-3}$ |
| (001), PZT-5A* | 338 | 14.7 | 43.1 | $40.1 \times 10^{-3}$ |

The general solution to (6) is

$$i(x) = A \cosh(\alpha x) + B \sinh(\alpha x) + I/2. \quad (9)$$

Using the boundary conditions (5), the constants $A$ and $B$ are determined to complete the solution:

$$i(\xi) = \frac{I}{2}\left[1 - \frac{\sinh(\varphi\xi)}{\sinh(\varphi)}\right] \quad (10a)$$

$$i'(\xi) = i(-\xi) \quad (10b)$$

where

$$\varphi \triangleq \frac{\alpha w}{2} \text{ is complex phase factor}$$

and

$$\xi \triangleq \frac{2x}{w} \text{ is a normalized aperture coordinate.}$$

From (1) and (4) the voltage is found to be

$$v(\xi) = \frac{I}{2}\frac{\alpha}{y}\frac{\cosh(\varphi\xi)}{\sinh(\varphi)}. \quad (11)$$

As expected, the inherent symmetry of the electrode structure about the aperture center is exhibited by the solutions (10) and (11).

The solutions for $v(x)$ and $i(x)$ are complex numbers because of the phase shifts introduced by the effective series $R$, shunt $C$ network. The phase of the acoustic radiation will be directly related to the phase of the electrode voltage $v(x)$. If $v(x)$ is not constant, then the acoustic radiation will not be of constant amplitude or uniform phase across the transducer aperture. The critical parameter will be $\varphi$ the product of $\alpha$, the characteristic wavenumber of the distributed $RC$ network, and half aperture, $w/2$. If $\varphi$ is small, then

$$i_0(\xi) \triangleq \lim_{\varphi\to 0} i(\xi) = \frac{I}{2}(1 - \xi) \quad (12a)$$

$$i_0'(\xi) \triangleq \lim_{\varphi\to 0} i'(\xi) = \frac{I}{2}(1 + \xi) \quad (12b)$$

and

$$v_0(\xi) = \frac{I}{wy} = V \text{ electrode terminal voltage.} \quad (13)$$

Thus if the series conduction resistance *or* aperture is sufficiently small, then $\varphi$ is small and the current and voltage reduce to their expected values for $\rho_s$ identically equal to zero.

The effects of series conduction losses are therefore dependent upon aperture width as well and not the metallization sheet resistance alone. This occurs because the distributed $RC$ network transforms shunt admittances through series impedances introducing a net phase shift dependent upon the overall length of the network and the propagation constant $\alpha$.

In reference to the general solutions (10) and (11) it should be noted that both $i(x)$ and $v(x)$ are referred to the assumed source current $I$. The actual terminal voltage $V$ will be related to $I$ and the network parameters through an equivalent impedance $Z$ which will be derived in the section on terminal properties. The functional dependence within the aperture will not be changed by the normalization even though the impedance will be a function of the overall aperture width.

The nature of the voltage and current distributions is illustrated in Figs. 2 and 3, respectively. The magnitude of the electrode voltage $\delta_V$ is normalized to the terminal voltage $V$ and its phase $\Delta\theta$ is referenced to the value at the center of the aperture. For low values of sheet resistance the electrode voltage approaches the terminal voltage in magnitude and phase. For finite sheet resistance, the voltage distribution becomes nonuniform and the phase is no longer constant along the aperture. The effect upon the excited wave is to distort the wavefront amplitude and phase. The inefficiency of high series conduction resistance is apparent by the reduction of the electrode voltage from the applied terminal voltage $V$.

The magnitude of the current distribution, $\delta_i$ and $\delta_i'$, normalized by $I$, is shown in Fig. 3 for one value of sheet resistance and two apertures. For low sheet resistance or

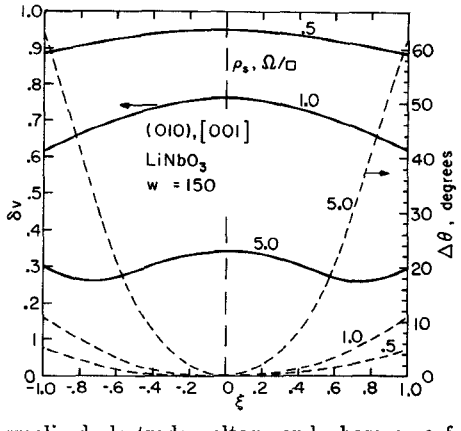


Fig. 2. Normalized electrode voltage and phase as a function of normalized aperture. The phase is relative to that at the center of the aperture.

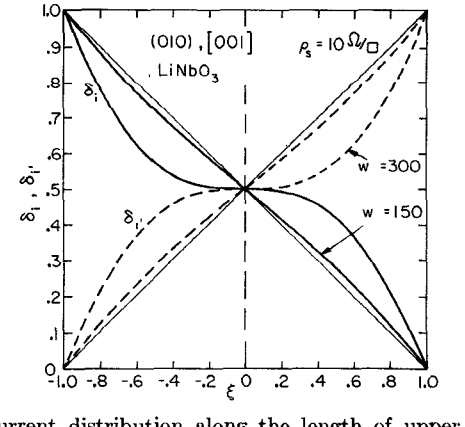


Fig. 3. Current distribution along the length of upper electrode $\delta_i$ and lower electrode $\delta_i'$ normalized to the input current $I$.

small apertures the current distribution is nearly linear and approaches the diagonal straight lines of (12). For higher sheet resistance, the series voltage drop causes the upper electrode current to transfer to the lower electrode at a faster rate and hence more near the ends of the electrode. At all positions in the aperture the upper and lower electrode currents must add to the total current $I$. The current distributions are thus antisymmetric about the aperture center and current values $I/2$, whereas the voltage is symmetric about the aperture center.

### D. Terminal Properties

Because of the physical size of IDT structures the current and voltage distributions within the electrodes are generally inaccessible and the net terminal effects become of primary interest. As stated before, the voltage distribution is not simply related to the terminal voltage $V$ because of the distributed circuit. Whereas a current $I$ was chosen as the independent variable for analysis purposes, the terminal voltage $V$ is more convenient as the independent variable for the purpose of interpreting conduction effects upon terminal properties. A general approach will be used to find the terminal impedances and equivalent circuit employing conservation of energy or power flow. By accounting for the power flow within the distributed structure and its integrated result, an equivalent impedance may be assigned at the terminals. The quantities of interest are the effective series resistance not associated with acoustic radiation, the effective series radiation resistance, and finally the series equivalent of the shunt reactance.

### E. Effective Series Conduction Resistance

Because of the nonuniform current distribution along each electrode, the apparent conduction resistance is in general not simply related to the metallization sheet resistance. However, an equivalent lumped element electrode resistance may be defined from the net terminal conduction power loss

$$P_c = \tfrac{1}{2} \mid I \mid^2 R_e \tag{14}$$

where $R_e$ is the effective series conductance resistance and $I$ is the electrode current.

The conduction power density, within the aperture, for the top electrode of Fig. 1 is just

$$P_c(x) = \tfrac{1}{2}\rho_c \mid i(x) \mid^2.$$

Thus the total electrode power loss, for both top and bottom electrodes, is obtained by integrating over the aperture

$$p_c = 2(\tfrac{1}{2}\rho_c)\int_{-w/2}^{w/2} \mid i(x) \mid^2 dx. \tag{15}$$

The leading factor of 2 in (15) is used to account for the loss in the lower electrode because of the symmetry between $i'(x)$ and $i(x)$. From (15) the integrated power is obtained:

$$P_c = \tfrac{1}{2}I^2(\tfrac{2}{3}\rho_c w)\eta_e \tag{16}$$

where

$$\eta_e = \frac{3}{4}\left[1 + \frac{[\sinh(w\alpha_r)]/w\alpha_r - [\sin(w\alpha_i)]/w\alpha_i}{\cosh(w\alpha_r) - \cos(w\alpha_i)}\right] \tag{17}$$

and

$$\alpha = \alpha_r + j\alpha_i.$$

The factor $\eta_e$ has the property that $\eta_e \to 1$ when $\varphi \to 0$. Thus from (14) and (16)

$$R_e = R_{e0}\eta_e \tag{18}$$

where

$$R_{e0} = \tfrac{2}{3}\rho_c w. \tag{19}$$

To first order, the electrode resistance is just $R_{e0}$ and simply related to the metallization sheet resistance through the relation

$$\rho_c = 4\rho_s\,\Omega/\lambda_0$$

where $\rho_s$ is the sheet resistance (ohms per square) and $\lambda_0$ is the electrode period. These relations hold for $\lambda_0/4$ or two $\lambda_0/8$ electrode pairs.

The expression for $R_{e0}$ (19) may also be inferred from the current distributions given in (12) through the integration in (15). For the usual materials, quartz, $LiNbO_3$, and $Bi_{12}GeO_{20}$, for apertures less than 500 wavelengths, and for sheet resistances less than 10 $\Omega/\square$, it is found that the series loss resistance is not strongly transformed by the distributed network and is simply equal to $R_{e0}$. Values of $R_e$ for apertures and sheet resistances greater than 500 and 10 $\Omega/\square$, respectively, are not considered likely for interdigital structures.

### F. Effective Radiation Impedance or Admittance

The radiation resistance or conductance may be defined as an equivalent terminal property in a manner similar to the series conduction resistance through the net power radiated acoustically. The complex power density in the shunt elements is given by

$$p_s(x) = \tfrac{1}{2}y^* \mid v(x) \mid^2. \tag{20}$$

The integrated power is obtained from (20) and (11):

$$P_s = \frac{1}{2}\left[\frac{1}{w}\frac{y^*}{\mid y \mid^2}\right]\eta_a I^2 \tag{21}$$

where

$$\eta_a = \left|\frac{\alpha w}{2}\right|^2 \left[\frac{[\sinh(\alpha_r w)]/\alpha_r w + [\sin(\alpha_i w)]/\alpha_i w}{\cosh(\alpha_r w) - \cos(\alpha_i w)}\right].$$

The factor $\eta_a$ has the property that $\eta_a \to 1$ as $\varphi \to 0$ similar to $\eta_e$ and thus gives the higher order dependence of radiation impedance upon aperture. From (21), the terminal series equivalent impedance of the distributed shunt elements may be inferred as

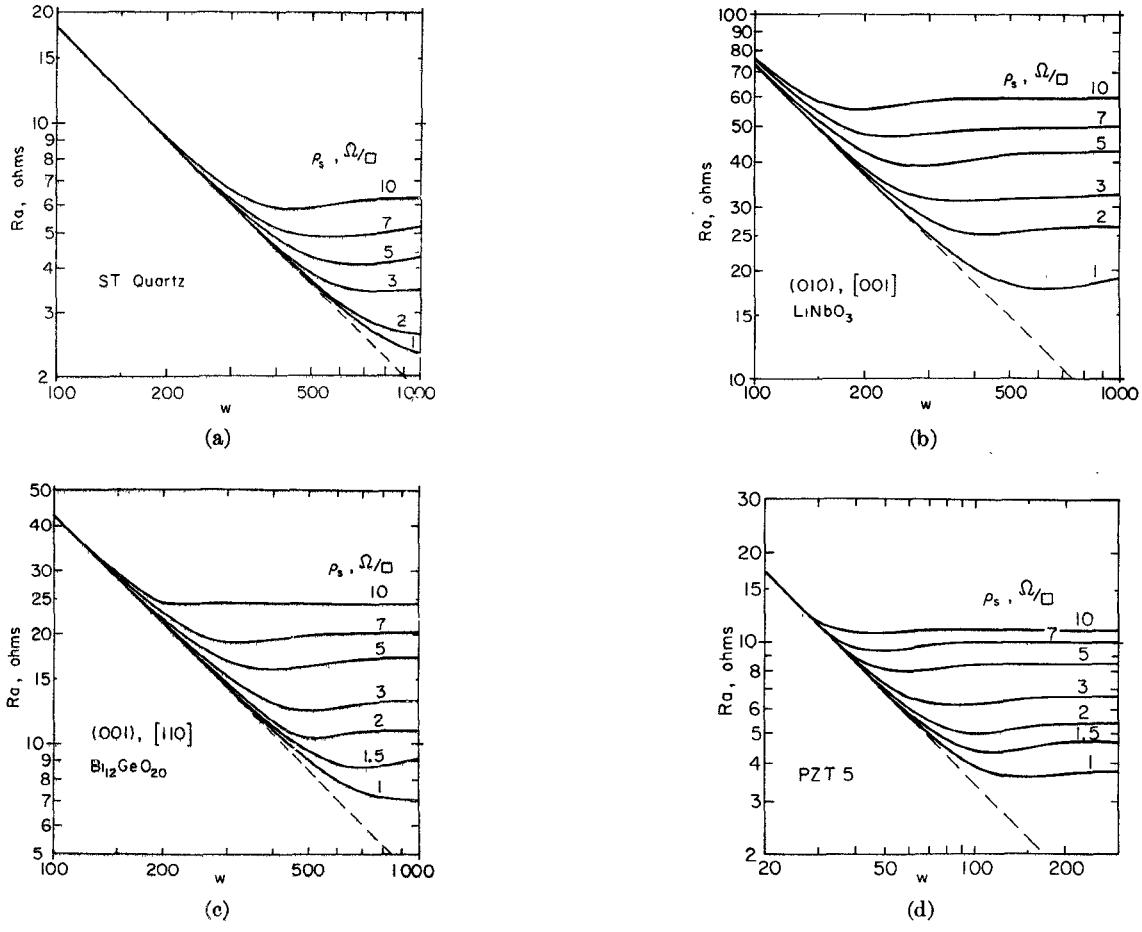


Fig. 4. Radiation resistance as a function of electrode overlap or aperture. The dashed line represents the characteristic when $\rho_s = 0$. (a) ST quartz. (b) YZ $LiNbO_3$. (c) Z cut [110] $Bi_{12}GeO_{20}$. (d) PZT-5A.

$$Z_s = \frac{1}{w} \frac{y^*}{|y|^2} \eta_a \tag{22}$$

or

$$Z_s = \frac{z}{w} \eta_a$$

where $z$ is the series equivalent of distributed impedance (ohms·$\lambda_0$) of shunt elements.

The terminal radiation resistance is then

$$R_a = \frac{\rho_a}{w} \eta_a$$

where $\rho_a$ is the distributed radiation resistance (ohms·$\lambda_0$) and the reactance is just

$$X = R_a Q_a$$

where

$$Q_a = \text{radiation } Q.$$

In the limit that $\varphi \to 0$, due to low series resistance $\rho_s$ and/or small aperture $w$, the finger pair series radiation resistance becomes, in first order,

$$R_a = \frac{\rho_a}{w}.$$

Values of radiation resistance have been calculated using the data in Table I for several materials representing a range of $\rho_a$ and $Q_a$ parameters. The calculated results are shown in Fig. 4 for ST quartz, YZ $LiNbO_3$, (001) [110] $Bi_{12}GeO_{20}$, and PZT5A.[1] Those materials with high dielectric constant exhibit a departure from the normal inverse falloff at a smaller aperture for the same metallization sheet resistance. The transformation in radiation resistance from the $1/w$ dependence occurs for an aperture value of

$$w \simeq 2/|\alpha|.$$

The phase factor $\alpha$ varies as the square root of the sheet resistance and shifts the departure point to smaller apertures as shown in Fig. 4.

Based upon the equivalent circuit of Fig. 5(a) an electrode pair efficiency may be calculated as

$$\eta = -10 \log_{10} (1 + R_e/R_a)$$

which is the ratio of power dissipated in useful acoustic radiation to the total dissipated power. The efficiency factor is shown in Fig. 6 for ST quartz and YZ $LiNbO_3$ as a function of aperture with sheet resistance as a parameter.

[1] PZT-5A is a registered trade name of Clevite Corporation.

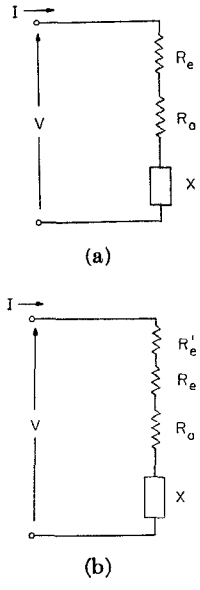


Fig. 5. Electrical equivalent circuits. (a) Electrode pair without additional series loss. (b) Weighted aperture with external metallization loss $R_e'$.

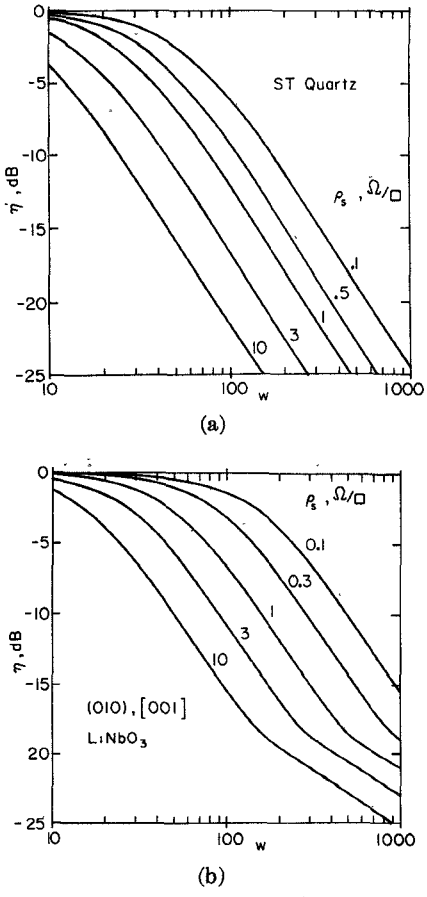


Fig. 6. Electrode efficiency in decibels as a function of aperture for the equivalent circuit of Fig. 5(a). (a) ST quartz. (b) YZ $LiNbO_3$.

Lithium niobate exhibits a somewhat higher efficiency because its $\rho_a$ is larger than that of quartz. Thus a larger aperture is required to reduce $R_a$ and increase $R_e$ to the point where $R_e$ is larger and dissipates the most power. The change in slope for larger apertures in $LiNbO_3$ is due to the fact that $R_a$ no longer decreases inversely with $w$ but instead remains relatively constant. In an ST quartz tapped delay line, a tap with $w = 100$ and $0.5\,\Omega/\square$ metallization would exhibit an additional 9-dB attenuation due to conduction losses.

### G. Aperture Weighting

In relation to tapped delay lines or frequency filter design it is often necessary to weight the aperture of individual taps or electrodes in an array. The usual manner is to employ a constant length electrode and to weight the electrode by the amount of electrode overlap. This gives rise to a radiating region which is connected to the bonding pad or electrode terminal by a metallized strip whose length depends upon the aperture width. The electrical equivalent circuit is shown in Fig. 5(a) where $R_e'$ represents the resistance of the electrodes outside the radiating aperture (overlap region) and $R_e$ is the effective electrode resistance for the aperture region. For the case of zero sheet resistance, both $R_e'$ and $R_e$ are zero, and only $R_a$ and $X$ have finite values. Since $R_a$ and $X$ have the same dependence upon $w$, their ratio $X/R$ is independent of aperture and thus the phase of the radiated wavefront is independent of aperture. If however, $\rho_s \neq 0$, then the ratio of $X$ to the total series resistance is no longer independent of aperture. Under these circumstances an attempt to amplitude weight also produces a phase weighting.

The expressions for the elements in the equivalent circuit are

$$R_e' = 4\rho_s w_0\left(1 - \frac{w}{w_0}\right)$$

$$R_e = \tfrac{8}{3}\rho_s \eta_e w_0 \left(\frac{w}{w_0}\right)$$

$$R_a = \frac{\rho_a \eta_a}{w_0}\left(\frac{w}{w_0}\right)^{-1}$$

$$X = Q_a R_a$$

where $w_0$ is the reference aperture and $w$ is the weighted aperture.

An effective aperture weighting factor $\delta_P$ may be defined as

$$\delta_P = \frac{P(w)}{P(w_0)}$$

where $P$ is the power radiated into acoustic waves.

In the absence of loss,

$$\delta_P(\rho_s = 0) = w/w_0.$$

Several cases have been calculated using a reference aperture of 100 wavelengths and are shown in Fig. 7. The extreme cases are for a rather large sheet resistance of 10 $\Omega/\square$, in Fig. 7(a). The case of $LiNbO_3$ indicates that there is relatively little change in the effective weighting until the overlap is less than 30 percent. This

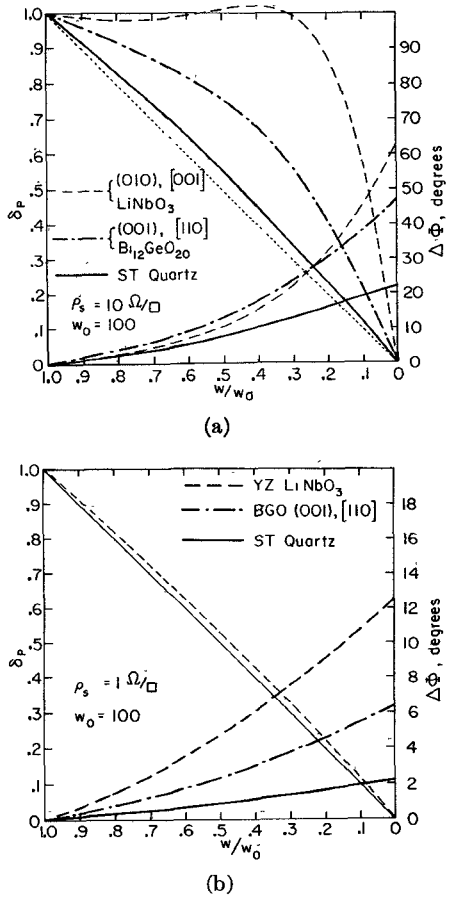


Fig. 7. Effective aperture weighting, $\delta_P$ as a function of electrode overlap weighting $w/w_0$. The dashed line $\delta_P = w/w_0$ is for the case $\rho_s = 0$. (a) Case for $\rho_s = 10\ \Omega/\square$. (b) $\rho_s = 1\ \Omega/\square$ sheet resistance.

insensitivity to aperture is due to the fact that as $w$ decreases, $R_a$ increases, and the loss resistance decreases. Since the transducer becomes more efficient at a smaller aperture more power is radiated and compensates the decrease in aperture. The phase shift $\Delta\Phi$ is the phase difference between the aperture $w$ and aperture $w_0$ transducer. This indicates that a phase error is introduced by amplitude weighting. These effects are less pronounced for low dielectric constant and lower coupling coefficient materials. For quartz, the capacitive reactance is much larger than $R_a$ or the series loss resistance and therefore has the effect of driving the electrodes with a current source whose value is nearly proportional to the aperture $w$. The phase shift is still pronounced even in quartz because the series resistance is determined largely by series loss and thus the ratio of $X$ to total resistance exhibits a $w^2$ dependence. For lower sheet resistances, Fig. 7(b), the effective weighting is nearly $w/w_0$ to first order but the phase shift is still present.

## III. CONCLUSION

A theory describing the effects of finite conduction loss in the metallization of an interdigital electrode pair is derived from an equivalent circuit representing a differential width in the aperture. From the resulting solutions the voltage and current distributions were found which showed significant departures from ideal when the distributed $RC$ circuit phase exceeded zero. The theory thus establishes a criterion for determining the maximum allowable sheet resistance which may be employed for a given substrate material and still maintain uniform amplitude and phase distribution across the aperture. An extension of the solutions to derive lumped terminal impedances and an equivalent circuit give quantitative information as to the radiation resistance, reactance, and loss resistance as a function of aperture and material parameters. It is found that the series radiation resistance departs from an inverse aperture width dependence at an aperture value of approximately $2/|\varphi|$ where $\varphi$ is the complex phase factor for the distributed $RC$ circuit. Substrate materials with high dielectric constant show the greatest $RC$ circuit transformations due to their larger phase factor. Application of the theory to transducer efficiency and effective weighting show that as the radiation resistance decreases with aperture the series loss increases to the point where more power is dissipated in the loss elements than in useful radiation. The theory shows that even low values of sheet resistance will produce phase errors when weighted sections are compared.

The theory has not been applied to transducer sections composed of more than one electrode pair. Such a procedure would be highly dependent upon the method of cascading elements into a given array. In any case, the series conduction loss is a factor associated with the metallization of the electrode capacitance and not the acoustic radiation as such. It is expected that the series loss would scale just as the capacitive reactance in a transducer as it must do for a simple capacitor with lossy metallization.

Experimental measurements have not been conducted to actually measure the current and voltage distribution along an interdigital structure. The physical size and impedance values rule out any meaningful measurements. Measurements upon tapped delay lines have proved inconclusive because of the unknown quantitive effects due to acoustic attenuation and beam diffraction.

## REFERENCES

[1] J. J. Campbell and W. R. Jones, "A method for estimating optimal crystal cuts and propagation directions for excitation of piezoelectric surface waves," *IEEE Trans. Sonics Ultrason.*, vol. SU-15, pp. 209–217, Oct. 1968.

[2] K. M. Lakin, "Perturbation theory for electromagnetic coupling to elastic surface waves on piezoelectric substrates," *J. Appl. Phys.*, vol. 42, pp. 899–906, Mar. 1971.

[3] D. Penunuri and K. M. Lakin, "Propagation of surface wave in anisotropic substrates," in *Proc. 1972 IEEE Ultrasonics Symp.*, pp. 328–332.

[4] ——, "Surface acoustic wave velocities of isotropic metal films on selected cuts of $Bi_{12}GeO_{20}$, quartz, $Al_2O_3$ and $LiNbO_3$," *IEEE Trans. Sonics Ultrason.*, to be published.

[5] W. R. Smith *et al.*, "Analysis of interdigital surface wave transducers by use of an equivalent circuit model," *IEEE Trans. Microwave Theory Tech. (Special Issue on Microwave Acoustics)*, vol. MTT-17, pp. 856–864, Nov. 1969.

[6] a) A. J. Slobodnik, Jr., and E. D. Conway, *Microwave Acoustics Handbook*, Air Force Cambridge Res. Lab., AFCRL-70-0164, Bedford, Mass., Mar. 1970.
b) A. J. Slobodnik and J. C. Sethares, *Measurement of the Elastic, Piezoelectric, and Dielectric Constants of $Bi_{12}GeO_{20}$*, Air Force Cambridge Res. Lab., AFCRL-71-0570, Bedford, Mass., Nov. 1971.
c) *Piezoelectric Technology Data for Designers*, Clevite Corp., Bedford, Ohio, 1965.